AMERICAN SOCIETY FOR MICROBIOLOGY | Infection and Immunity®

MOLECULAR PATHOGENESIS

The LiaFSR Transcriptome Reveals an Interconnected Regulatory Network in Group A *Streptococcus*

Misu A. Sanson,[a] Luis Alberto Vega,[a] Brittany Shah,[a] Shrijana Regmi,[a] M. Belen Cubria,[a] Nicola Horstmann,[b,c] Samuel A. Shelburne III,[b,c] Anthony R. Flores[a]

[a]Division of Infectious Diseases, Department of Pediatrics, Center for Antimicrobial Resistance and Microbial Genomics, McGovern Medical School, University of Texas Health Sciences Center at Houston, Houston, Texas, USA
[b]Department of Infectious Diseases, MD Anderson Cancer Center, Houston, Texas, USA
[c]Department of Genomic Medicine, MD Anderson Cancer Center, Houston, Texas, USA

ABSTRACT The mechanisms by which bacteria sense the host environment and alter gene expression are poorly understood. LiaFSR is a gene regulatory system unique to Gram-positive bacteria, including group A *Streptococcus* (GAS), and responds to cell envelope stress. We previously showed that LiaF acts as an inhibitor to LiaFSR activation in GAS. To better understand gene regulation associated with LiaFSR activation, we performed RNA sequencing on isogenic deletion mutants fixed in a LiaFSR "always on" (Δ*liaF*) or "always off" (Δ*liaR*) state. Transcriptome analyses of Δ*liaF* and Δ*liaR* in GAS showed near perfect inverse correlation, including the gene encoding the global transcriptional regulator SpxA2. In addition, mutant transcriptomes included genes encoding multiple virulence factors and showed substantial overlap with the CovRS regulon. Chromatin immunoprecipitation quantitative PCR demonstrated direct *spxA2* gene regulation following activation of the response regulator, LiaR. High SpxA2 levels as a result of LiaFSR activation were directly correlated with increased CovR-regulated virulence gene transcription. Furthermore, consistent with known virulence gene repression by phosphorylated CovR, elevated SpxA2 levels were inversely correlated with CovR phosphorylation. Despite increased transcription of several virulence factors, Δ*liaF* (high SpxA2) exhibited a paradoxical virulence phenotype in both *in vivo* mouse and *ex vivo* human blood models of disease. Likewise, despite decreased virulence factor transcription with Δ*liaR* (low SpxA2), increased virulence was observed in an *in vivo* mouse model of disease—a phenotype attributable, in part, to known SpxA2-associated *speB* transcription. Our findings provide evidence of a critical role of LiaFSR in sensing the host environment and suggest a potential mechanism for gene regulatory system cross talk shared by many Gram-positive pathogens.

KEYWORDS group A *Streptococcus*, gene regulation, membrane microdomain, two-component system, antimicrobial peptide, virulence

Streptococcus pyogenes (group A *Streptococcus* [GAS]) is responsible for >700 million infections worldwide annually (1). Capable of a remarkable breadth of disease phenotypes, GAS is the cause of relatively benign pharyngitis ("strep throat") and severe life-threatening diseases such as necrotizing fasciitis ("flesh-eating disease") and toxic shock syndrome. Until recently, the epidemiology of GAS disease had remained relatively stable over the past 20 years, with the incidence of severe invasive disease ranging between 3 and 5 cases per 100,000 persons (2, 3). However, beginning in 2017, national surveillance performed by the Centers for Disease Control and Prevention (CDC) showed a marked increase in invasive disease, which is currently >7 cases per 100,000 persons (4), underscoring our need to better understand the biology of this important human pathogen.

Citation Sanson MA, Vega LA, Shah B, Regmi S, Cubria MB, Horstmann N, Shelburne SA, III, Flores AR. 2021. The LiaFSR transcriptome reveals an interconnected regulatory network in group A *Streptococcus*. Infect Immun 89: e00215-21. https://doi.org/10.1128/IAI.00215-21.

Editor Nancy E. Freitag, University of Illinois at Chicago

Address correspondence to Anthony R. Flores, anthony.r.flores@uth.tmc.edu.

Received 20 April 2021
Returned for modification 25 May 2021
Accepted 2 August 2021
Accepted manuscript posted online 9 August 2021
Published 15 October 2021

The ability of GAS to elaborate such a broad array of disease phenotypes is dependent upon precise gene regulation in response to host stimuli. To accomplish this goal, the GAS genome harbors 13 two-component systems (TCSs) and several stand-alone regulators (5). TCSs generally consist of a membrane-bound sensor histidine kinase (HK) that, in response to a stimulus, activates via phosphotransfer a cognate response regulator (RR) (6). The most studied of the GAS TCS is the control of virulence, CovRS (7, 8). The GAS CovRS regulates approximately 10% of the GAS genome in response to host Mg^{2+} or the antimicrobial peptide LL-37 and includes virulence genes encoding capsule biosynthesis (*hasABC*), interleukin 8 (IL-8) protease (*prtS*, *spyCEP*), IgG protease (*mac-1*, *ideS*), streptokinase (*ska*), and NADase/streptolysin O (*nga*/*slo*) among others (9, 10). However, in contrast to typical HK/RR pairs, phosphorylated CovR acts primarily to repress virulence gene regulation. Thus, in the absence of CovS, CovR exists in a dephosphorylated state allowing increased expression (i.e., derepression) of target genes. Not surprisingly, invasive GAS strains are known to have a high frequency of inactivating mutations in *covS*, and such mutations have been shown to develop *in vivo* during human infection (11–13).

The LiaFSR three-component system (3CS) is well-known in Gram-positive bacteria to contribute to antimicrobial resistance (14, 15), but global gene regulation through LiaFSR is poorly defined in GAS. The Lia (lipid II interacting antibiotic) system responds to cell envelope stress induced by antibiotics or host molecules that target the cell envelope (e.g., LL-37) and is unique to *Firmicutes* (16). In addition to an HK (LiaS) and an RR (LiaR), LiaF is a membrane-bound protein that coordinates with LiaS through an as-yet-unknown mechanism to enhance (*Staphylococcus aureus*) (17) or inhibit (*Bacillus subtilis*, GAS) (18, 19) LiaS and, subsequently, LiaR activation. We recently described an intimate relationship between the membrane-bound proteins LiaS and LiaF with the GAS functional membrane microdomain (FMM), also known as ExPortal (19). In addition to colocalizing to the GAS ExPortal, our study showed that perturbation of ExPortal integrity through the action of cell envelope-active antimicrobials or the human antimicrobial peptide (AMP) human neutrophil peptide-1 (hNP-1) led to LiaF/LiaS dissociation and activation of the LiaFSR system. Moreover, in the absence of LiaF, the LiaR response regulator was constitutively phosphorylated, indicating that LiaF is an inhibitor of activation (19). However, the global gene regulatory changes resulting from LiaFSR activation are unknown.

Spx (suppressor of ClpP and ClpX) proteins are highly conserved transcriptional regulators that act by binding RNA polymerase and, similarly to LiaFSR, are unique to *Firmicutes* (20). Spx was first identified in *Bacillus* as a protein that bound specifically to the alpha subunit of RNA polymerase and acted as an antiactivator (21). More recently, data suggest that the GAS SpxA2 affects the ability of the stand-alone regulator RopB to bind to its target promoter, leading to decreased SpeB (cysteine protease) production (22). Interestingly, our early transcriptome studies identified *spxA2* as the most highly differentially expressed gene in a carrier mutant (single amino acid change in LiaS) (23), and data suggest direct LiaR regulation in *Streptococcus mutans* (24) and *Streptococcus agalactiae* (group B *Streptococcus* [GBS]) (25). Thus, one may postulate that global gene regulation through LiaFSR is made more complex through the actions of SpxA2. Here, we extend our previous studies to define the regulon of LiaFSR in GAS. In so doing, we have uncovered a complex regulatory network that extends beyond LiaFSR and potentially links multiple regulatory systems in GAS.

RESULTS

Constitutive LiaFSR activation or repression reveals altered CovR-regulated gene transcription. Our previous studies confirmed that the accessory protein LiaF acts to inhibit the activity of LiaFSR (19). Specifically, we showed that in the absence of LiaF, LiaR was highly phosphorylated, indicating high-level LiaS activity. Thus, in order to begin to define the LiaFSR regulon, we used RNA sequencing (RNA-seq) to compare transcriptomes between the parental serotype M3 strain MGAS10870 and isogenic mutant strains lacking LiaR (Δ*liaR*, LiaFSR inactive) or LiaF (Δ*liaF*, LiaFSR active) during

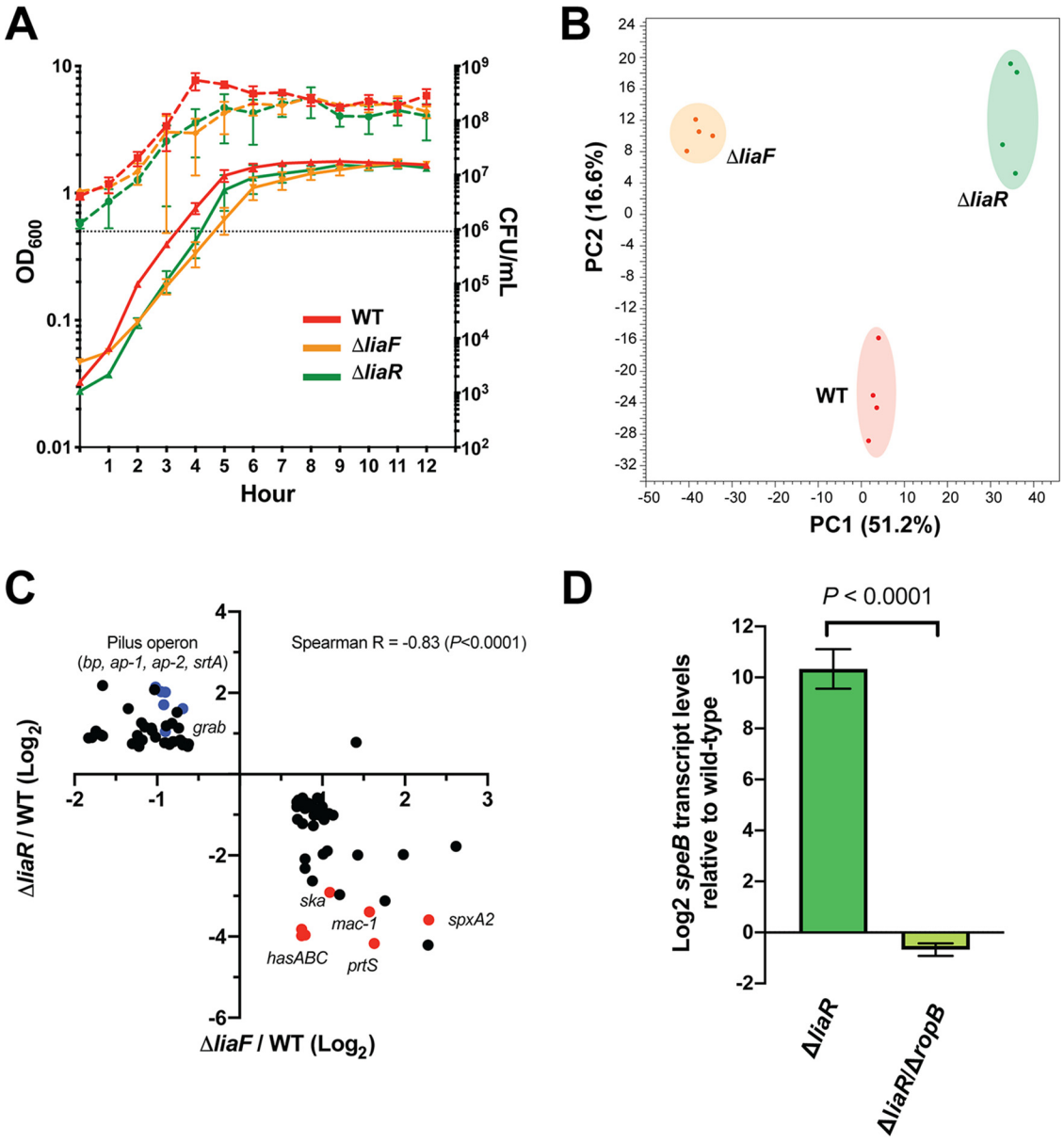

FIG 1 Transcriptomes of Δ*liaF* and Δ*liaR* mutants reveal LiaFSR influence on virulence gene regulation in GAS. (A) Growth phenotypes of parental (WT, red) and isogenic mutant (Δ*liaF*, orange; Δ*liaR*, green) strains following growth *in vitro* in nutrient-rich medium. Growth was performed in biological triplicates and measured by absorbance (OD_{600}, left *y* axis, solid lines) and CFU (CFU/ml, right *y* axis, dashed lines). (B) Principal-component analysis (PCA) of parental and isogenic mutant strain transcriptomes (mid-exponential growth in nutrient-rich medium). Biological replicates (colored dots) are indicated for each strain. (C) Correlation plot of 88 significantly ($P < 0.05$, Bonferroni correction) differentially expressed genes (≥1.5-fold, relative to the parental strain) shared between the Δ*liaF* (*x* axis) and Δ*liaR* (*y* axis) transcriptomes. Log_2 values are plotted, and genes listed in Table 1 are colored (blue or red) and labeled. Red and blue labels indicate genes involved in adherence (blue) or virulence (red). (D) Quantitative real-time PCR comparing *speB* transcription in the Δ*liaR* and the Δ*liaR* Δ*ropB* mutants (relative to the parental strain). Assays were performed in triplicates. *P* value was determined using the Student's *t* test.

growth in a standard laboratory medium. Prior to initiating RNA-seq studies, we demonstrated a lack of growth differences between parental and isogenic mutant strains (Fig. 1A). While subtle differences in growth were observed, we did not identify significantly different CFU at the time cells were harvested for RNA-seq (optical density at 600 nm [OD_{600}] of ~0.5). In addition, alteration of LiaFSR activity has previously been shown to affect antimicrobial susceptibility in *Enterococcus* (14, 15). However, we observed no significant changes in susceptibility patterns in isogenic mutants

TABLE 1 Select differentially expressed genes in Δ*liaF* and Δ*liaR* isogenic mutants relative to that in the parental strain, MGAS10870

Locus[a]	Gene[b]	Predicted product	Fold change[c]	
			Δ*liaF*	Δ*liaR*
	speC	Streptococcal pyrogenic exotoxin, C	−3.35	2.08
SpyM3_0098	*ap-1*	Pilus, accessory protein-1	−2.03	4.40
SpyM3_0099	*srtA1*	Pilus, sortase A1	−1.87	4.06
SpyM3_0100	*tee3*	Pilus, backbone protein (tee)	−1.93	4.07
SpyM3_0101	*srtA2*	Pilus, sortase A2	−1.89	3.26
SpyM3_0102	*ap-2*	Pilus, accessory protein-2	−1.62	3.05
SpyM3_0103	*msmR*	Multiple sugar metabolism regulator	−1.78	
SpyM3_0298	***prtS***	IL-8 protease (PrtS/SpyCEP)	3.09	−17.98
SpyM3_0583	***mac-1***	IgG protease (Mac-1/IdeS)	2.97	−10.50
SpyM3_1032	*grab*	Protein G-related α2-macroglobulin-binding protein	−1.87	2.07
SpyM3_1301	*speA3*	Streptococcal pyrogenic exotoxin, A3	2.70	−3.96
SpyM3_1409	*sdn*	Streptodornase (Sdn)	−3.64	
SpyM3_1698	***ska***	Streptokinase A precursor	2.13	−7.54
SpyM3_1728	*mga*	M protein trans-acting positive regulator	1.62	−2.16
SpyM3_1742	*speB*	Secreted cysteine protease		432.03
SpyM3_1744	*ropB*	Regulator of proteinase B	−1.76	2.38
SpyM3_1799	*spxA2*	Transcriptional regulator Spx	4.89	−12.07
SpyM3_1851	***hasA***	Hyaluronan synthase (capsule)	1.73	−15.54
SpyM3_1852	***hasB***	UDP-glucose 6-dehydrogenase (capsule)	1.68	−15.81
SpyM3_1853	***hasC***	UDP-glucose pyrophosphorylase (capsule)	1.68	−14.10

[a]Locus tag designation in the reference genome MGAS315.
[b]Gene names in bold font indicate predicted or known regulation by CovRS.
[c]Values for Δ*liaF* and Δ*liaR* are fold-change relative to the parental strain, MGAS10870. Only fold-change values with a *P* value <0.05 (Bonferroni corrected for multiple comparisons) are shown in the table.

compared to that in the parental strain, including cell wall/envelope active agents (see Table S1 in the supplemental material). Principal-component analysis (PCA) of parental and isogenic mutant strains indicated tight clustering between biological replicates and mutant transcriptomes distinct from those of the parental strain and each other (Fig. 1B). Analysis of differential gene expression (DGE) relative to the parental strain (≥1.5-fold change, $P < 0.05$ adjusted for multiple comparisons, core genome only, excluding phage and other mobile elements) showed substantial overlap of the mutant strain transcriptomes (see Table S2). Examination of the Δ*liaF* transcriptome showed the largest influence on the GAS genome affecting 207 genes compared to 148 differentially expressed genes in the Δ*liaR* mutant (Table S2). The two isogenic deletion mutants, Δ*liaR* and Δ*liaF*, shared 84 differentially expressed genes (Table S2). Consistent with LiaF acting as an inhibitor of the LiaFSR system, we observed near perfect inverse correlation between those genes shared by Δ*liaF* (LiaFSR active, high LiaR phosphorylation) and Δ*liaR* (LiaFSR inactive, absence of LiaR) transcriptomes (Fig. 1C). For example, in the absence of LiaR, *spxA2* transcription (predicted to be regulated by LiaR) was reduced >12-fold (LiaFSR inactive) but was increased nearly 5-fold in the absence of LiaF (LiaFSR active) (Fig. 1C; Table 1).

Significant DGE in both the Δ*liaR* and Δ*liaF* mutants relative to expression in the parental strain included several genes known to encode key virulence factors (Table 1). For example, the entire pilus operon (SpyM3_0098 to SpyM3_0102), previously shown to be affected in the carrier LiaS mutant (23), was significantly downregulated in the Δ*liaF* mutant but significantly upregulated in the Δ*liaR* mutant (Table 1). Perhaps most surprisingly, when we examined the most highly differentially expressed genes within the mutant transcriptomes, we identified several genes known to be regulated by the CovRS TCS (Table 1; Table S2). Genes encoding capsule biosynthesis (*hasABC*), IL-8 protease (*prtS*, *spyCEP*), IgG protease (*mac-1*, *ideS*), and streptokinase (*ska*) were all significantly decreased in the Δ*liaR* mutant and significantly increased in the Δ*liaF* mutant transcriptomes relative to expression in the parental strain (Fig. 1C, red dots; Table 1).

In addition, we observed significantly increased transcription of genes involved in adherence (e.g., grab [protein G-related alpha-2-macroglobulin-binding protein] and pilus operon) in the Δ*liaR* mutants, while such genes were significantly decreased in the Δ*liaF* mutant (Fig. 1C, blue dots; Table 1).

The most highly differentially expressed gene in the Δ*liaR* mutant relative to expression in the parental strain was the gene encoding a cysteine protease, *speB* (+432-fold) (Table 1). However, transcript levels for *ropB*, encoding the major regulator for *speB*, were only modestly increased (Table 1), suggesting another mechanism contributing to the markedly increased *speB* transcription. Port et al. showed that *speB* transcription, in addition to being regulated by the stand-alone regulator RopB, was influenced by levels of SpxA2 (22). SpxA2 binds the alpha subunit of RNA polymerase to influence gene transcription (20). In the absence of SpxA2, GAS cells produced excessive amounts of SpeB, and it was proposed that SpxA2 may interfere with RopB binding to the *speB* promoter when SpxA2 is in high abundance (22). The effect was not seen in the absence of RopB, the major regulator for *speB* transcription, indicating that SpxA2 does not independently influence *speB* transcription (22). To assess the same possibility in the Δ*liaR* mutant, we generated a *ropB* deletion mutant in the Δ*liaR* background (Δ*liaR* Δ*ropB*) and compared *speB* transcript levels in mutant and parental strains. We observed significantly reduced *speB* transcription in the strain lacking *ropB* compared to that in the parental strain (Fig. 1D), indicating RopB is essential for the changes in *speB* transcription observed following LiaR inactivation.

LiaR directly regulates *spxA2* gene transcription in GAS. Previous studies in *Streptococcus mutans* showed direct transcriptional regulation of the *spxA2* homolog (*spxA*) by LiaR (24). In addition, in a transcriptome analysis in GBS strain A909 lacking *liaR*, the *spxA2* homolog was the most significantly differentially expressed gene, showing >26-fold reduced transcript level compared to that in the parental strain (25). An alignment comparing the GAS *spxA2*, *S. mutans spxB-spxA1*, and GBS *spxA* promoters indicates a relatively high level of conservation, including the predicted *S. mutans* LiaR binding motif (LiaR motif A) (Fig. 2A). However, relative to that in *S. mutans*, the promoters in GAS and GBS were extended and included additional upstream predicted −10 and −35 motifs (Fig. 2A). Furthermore, using the MEME suite for motif identification (26), a second putative LiaR binding site was identified in the GAS extended promoter sequence but was absent in both GBS and *S. mutans* sequences (Fig. 2A, LiaR Motif B). Given the high degree of promoter homology at the known *S. mutans* LiaR binding site of the *spxA2* promoter, we hypothesized the LiaR directly regulates *spxA2* gene expression in GAS.

To demonstrate direct LiaR regulation of *spxA2* gene transcription in GAS, we used quantitative real-time PCR (qPCR) following chromatin immunoprecipitation (ChIP) to compare target DNA (*spxA2* promoter) enrichment between the wild type (MGAS10870) and the Δ*liaR* isogenic mutant strain. Consistent with increased LiaR phosphorylation following LiaFSR activation by bacitracin (BAC) (19), we observed significant enrichment of *spxA2* promoter motifs A and B following ChIP using LiaR-specific antibody only after activation with BAC (Fig. 2B). No enrichment was observed in the Δ*liaR* mutant or with the control target *tufA*, demonstrating specificity for DNA bound by LiaR (Fig. 2B). In addition to ChIP qPCR, we generated a mutant lacking *spxA2* in the Δ*liaR* background (Δ*liaR* Δ*spxA2*). Relative to the Δ*liaR* isogenic mutant, we did not observe significant differences in CovR-regulated virulence gene transcription in the double knockout (Fig. 2C). Together, these data indicate that LiaR is the major regulator of SpxA2 in GAS.

Transcriptional changes in CovRS-regulated genes correlate with changes in *spxA2* gene transcription and CovR phosphorylation. Given that *spxA2* is a major gene regulatory target following LiaFSR activation and that it was predicted that SpxA2 interferes with RopB activity (22), we next hypothesized that the observed changes in *spxA2* transcript level may not only influence *speB* but are associated with changes in CovRS-regulated gene transcription (Fig. 1C, red dots). Specifically, we hypothesized that if we altered SpxA2 levels in the wild type or the Δ*liaF* mutant, we would observe corresponding changes in CovRS-regulated virulence gene transcription. In the absence of

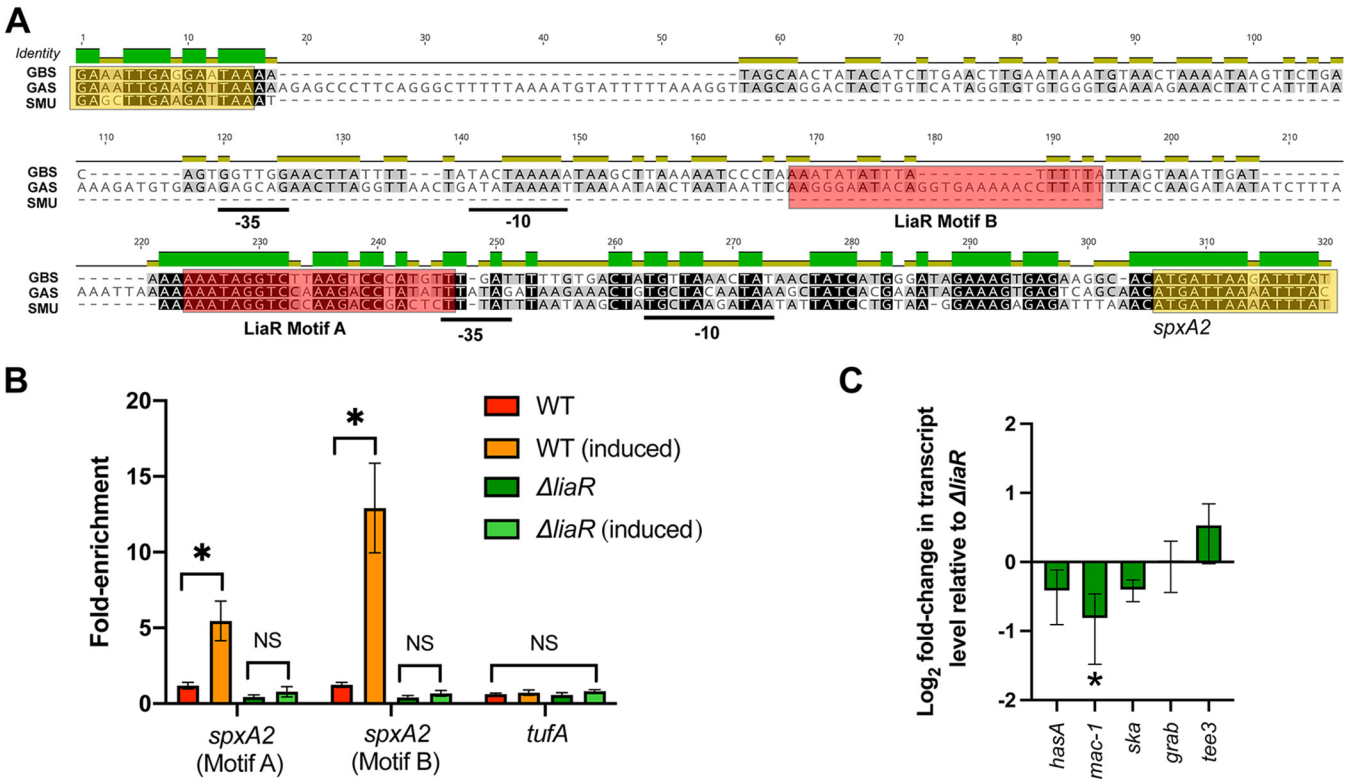

FIG 2 LiaR directly regulates *spxA2* gene expression in GAS. (A) Promoter alignment of *spxA2* homologs in GAS (strain MGAS10870), *S. mutans* ([SMU] strain UA159), and GBS (strain A909). Relative identity is provided above the sequence alignment (green indicates identical). Putative −10 and −35 boxes are underlined. Putative LiaR binding motifs are indicated by red shaded boxes. The 3′ terminal coding sequence for the upstream gene and 5′ coding sequence for *spxA2* are indicated by yellow boxes. (B) Chromatin immunoprecipitation (ChIP) quantitative real-time PCR (qPCR) derived from parental (WT) or Δ*liaR* isogenic mutant strains grown as described in Materials and Methods with or without bacitracin (induced). Primer/probe sequences used in qPCR are provided in Table S4 in the supplemental material. Fold-enrichment relative to the WT (uninduced) is shown on the *y* axis and the target is indicated on the *x* axis. *, $P < 0.05$ (Student's *t* test) on assays performed in biological triplicates; comparisons lacking significance are indicated (not significant [NS]). (C) Quantitative real-time PCR comparing target gene transcription of the Δ*liaR* Δ*spxA2* mutant relative to that in the Δ*liaR* mutant. Shown are transcript levels derived from biological triplicate samples grown *in vitro* to mid-exponential phase as described in Materials and Methods. *, $P < 0.05$ (Student's *t* test).

oxidative stress, SpxA2 is rapidly degraded by the ClpXP protease (20). We reasoned that deletion of *clpX* would serve to preserve SpxA2 and, if SpxA2 positively influences CovRS-regulated gene transcription, increase CovRS-regulated gene transcript levels in the wild-type background. In contrast, deletion of *spxA2* in the Δ*liaF* mutant (Δ*liaF* Δ*spxA2*) would essentially reverse gene transcription to levels observed in the Δ*liaR* mutant (Fig. 1C; Table S2). Given the known increased susceptibility to oxidative stress in the absence of SpxA2 (20, 22), we first assessed isogenic mutants following exposure to diamide (tetramethylazodicarboxamide), a compound that induces oxidative stress through S-thiolation (27). Following exposure to diamide, strains predicted to have low SpxA2 levels (Δ*liaR*, Δ*spxA2*, and Δ*liaF* Δ*spxA2* mutants) showed decreased survival compared to strains predicted to have high SpxA2 levels (Δ*liaF* and Δ*clpX* mutants) (Fig. S1). Importantly, these data are in support of a direct correlation between SpxA2 protein levels and *spxA2* transcription seen in the Δ*liaR* and Δ*liaF* mutants.

We next compared transcript levels of CovR-regulated genes (*hasA*, *mac-1*, and *ska*) (Table 1, bold font) predicted to be upregulated when SpxA2 levels are increased. In addition, we assayed genes encoding adhesins (*grab* and *tee3*) predicted to be upregulated when SpxA2 levels are decreased. As predicted by our hypothesis, under high SpxA2 conditions (Δ*liaF* and Δ*clpX*) we observed decreased *grab* and *tee3* but increased *mac-1* and *ska* gene transcript levels relative to those in the parental strain, while transcript levels for *hasA* were more variable (Fig. 3A, red and orange bars). In contrast, the transcription level patterns were completely reversed in the mutants

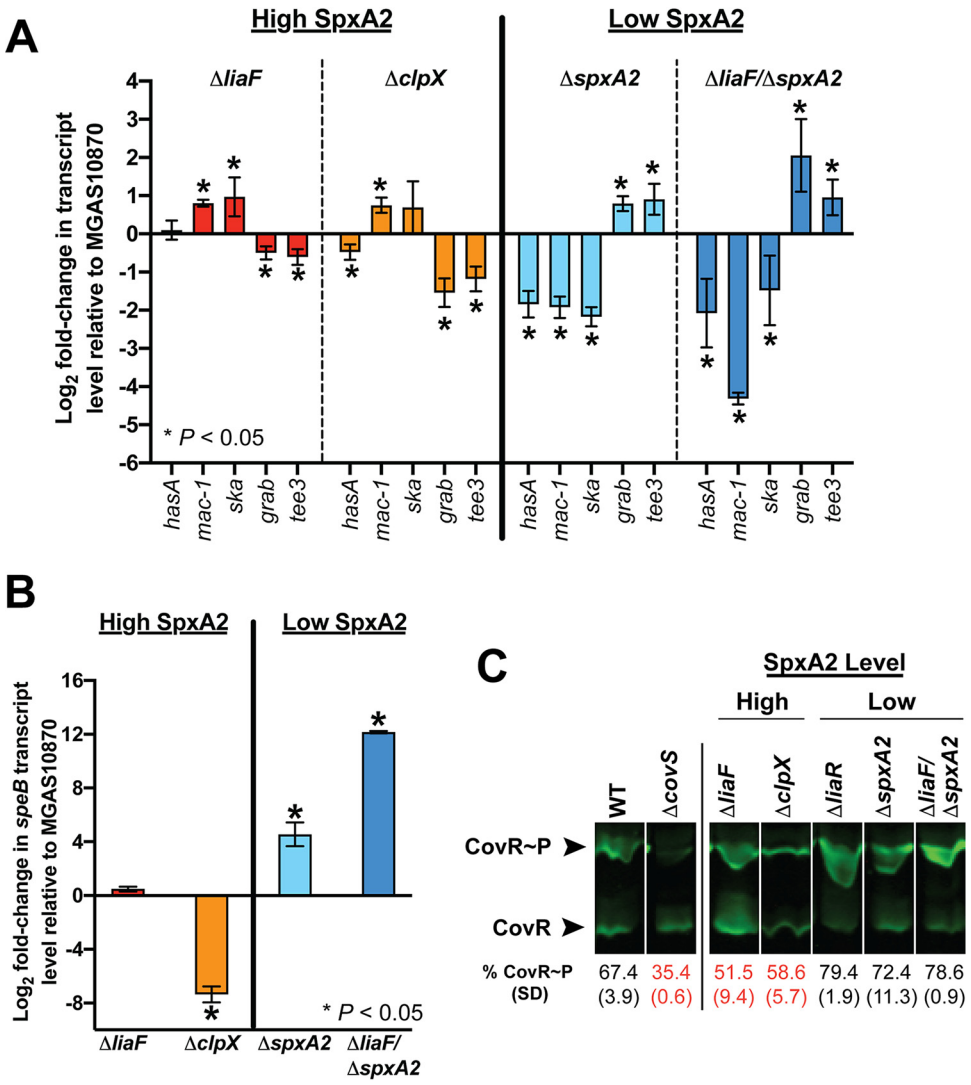

FIG 3 Virulence gene regulation in GAS correlates with SpxA2 levels. (A) Quantitative real-time PCR (qRT-PCR) of selected targets in isogenic mutants with high (Δ*liaF*, Δ*clpX*) or low (Δ*spxA2*, Δ*liaF* Δ*spxA2*) SpxA2 levels. Strains were grown in nutrient-rich medium identical to conditions used for RNA-seq studies (mid-exponential growth) and in biological quadruplicates. *, $P < 0.05$ (Student's *t* test). (B) qRT-PCR to assay *speB* transcript levels in isogenic mutant strains as in panel A. (C) Phos-Tag protein gel electrophoresis to assay CovR phosphorylation (CovR~P) in isogenic mutant strains with high or low SpxA2 levels. Levels of phosphorylation for each mutant are indicated (relative to the wild-type [WT] strain), with red text indicating decreased CovR~P relative to that in the WT.

lacking *spxA2* compared to those in mutants with high SpxA2 levels (Fig. 3A, light and dark blue bars). Consistent with the previous report showing an inverse association between SpxA2 level and *speB* expression (22), *speB* transcript levels were significantly upregulated in the absence of SpxA2 (Fig. 3B). Thus, these data indicate a direct association between SpxA2 and virulence gene expression and suggest potential SpxA2 interaction with multiple transcriptional regulators (e.g., RopB and CovR).

In contrast to most bacterial TCSs, the activation of CovS and increased CovR phosphorylation (CovR~P) results in repression (rather than activation) of target gene transcription (7). Next, we sought to determine whether there was an association between SpxA2 and CovR~P levels. Specifically, we hypothesized that CovR~P was also affected in the isogenic mutants (Δ*liaF* and Δ*liaR* mutants) and was inversely related to levels of SpxA2 (high SpxA2, low CovR~P, and derepression of virulence gene transcription). To test this possibility, we assayed CovR~P levels from parental and isogenic mutant GAS

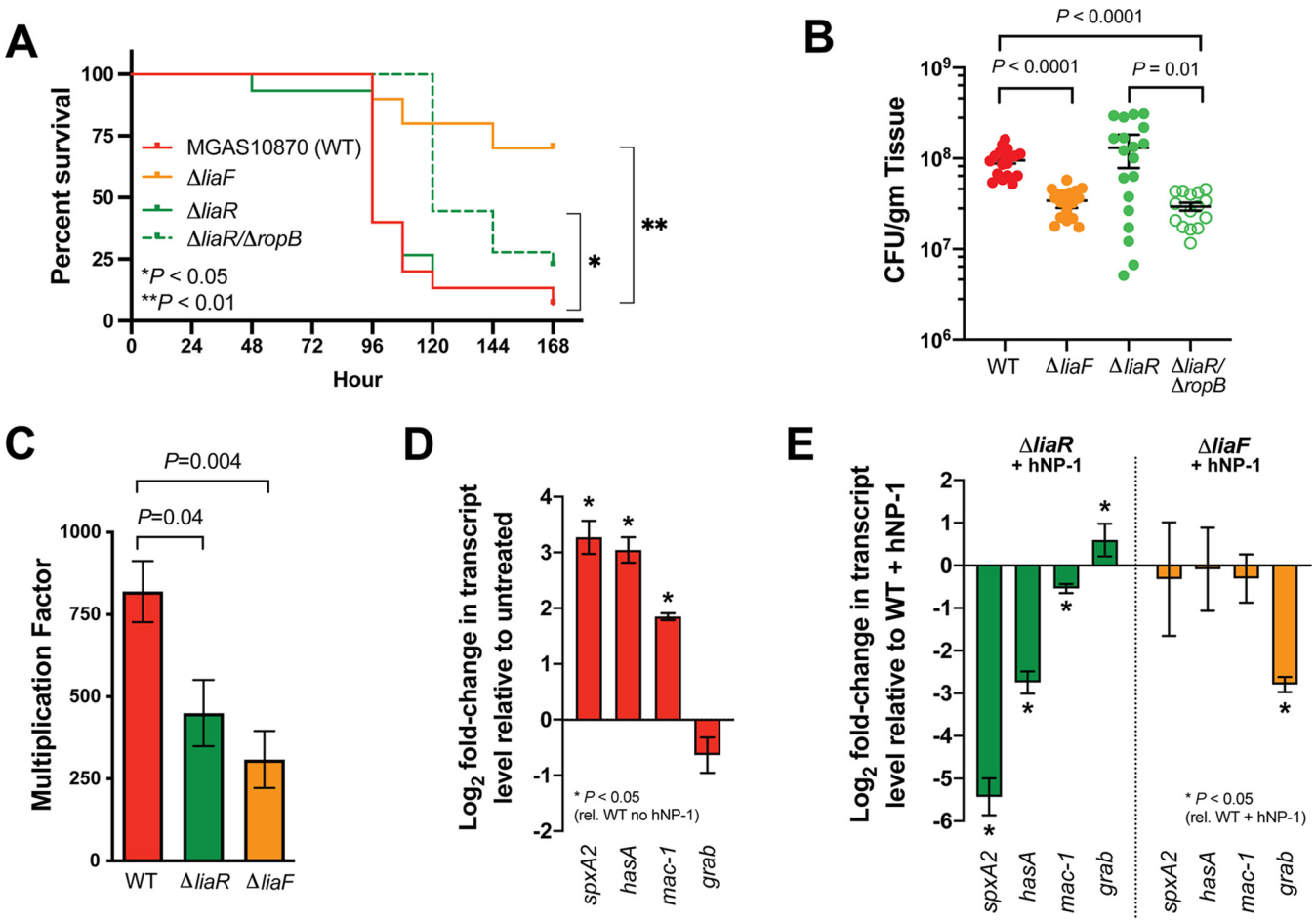

FIG 4 Isogenic mutants of *liaF* and *liaR* exhibit paradoxical virulence phenotypes compared to their respective transcriptomes. (A) Kaplan-Meier survival of mice (n = 15 per strain) infected with the WT, Δ*liaF*, Δ*liaR*, or double mutant Δ*liaR* Δ*ropB* strain. *P* values were determined by log rank. (B) Bacterial burden of same GAS strains as in panel A at 48 h postinfection. *P* values were determined by Mann-Whitney U test. (C) *Ex vivo* human bactericidal assays of WT (red), Δ*liaR* (green), or Δ*liaF* strain (2 independent donors performed in quadruplicates). *P* value was determined by Mann-Whitney U test. Quantitative real-time PCR of selected transcript targets in the wild-type strain MGAS10870 (D) or isogenic deletion strains (E) following exposure to hNP-1 *in vitro* as described in Materials and Methods. Log_2 fold change (*y* axis) for MGAS10870 (D) relative to the untreated control and for isogenic mutant strains treated with hNP-1 relative to the WT plus hNP-1 (E). *P* values were determined by Student's *t* test.

cells *in vivo* using Phos-Tag. We discovered that isogenic mutant strains with significantly reduced (Δ*liaR*) or absent (Δ*spxA2* strains) *spxA2* transcription exhibited increased *in vivo* CovR∼P (virulence gene repression) (Fig. 3C). In contrast, strains with significantly increased (Δ*liaF* or Δ*clpX* strains) SpxA2 levels displayed decreased *in vivo* CovR∼P (virulence gene derepression) (Fig. 3D). In summary, our data indicate that activation of LiaFSR results in increased SpxA2 that in turn alters CovR∼P and virulence gene transcription.

Paradoxical virulence *in vivo* and *ex vivo* phenotypes of isogenic mutants suggest critical roles of SpxA2 and ExPortal in GAS-host interaction. Given the observed overlap with the LiaFSR transcriptome and CovR-regulated gene expression, we hypothesized that constitutive activation of LiaFSR (Δ*liaF*) would result in increased virulence compared to that with constitutive repression of LiaFSR (Δ*liaR*) owing to differences in virulence gene transcript levels (Fig. 1C; Table S2). To begin testing our hypothesis, we compared Δ*liaF* and Δ*liaR* isogenic mutants in a mouse model of necrotizing fasciitis (28). Paradoxical to the predicted phenotype based on the transcriptome profile (Fig. 1C; Table S2), mice infected with the Δ*liaF* mutant exhibited significantly increased survival and decreased CFU recovery compared to the parental strain (Fig. 4A and B). Furthermore, and also contradictory to the predicted phenotype based on the *in vitro* transcriptome (Fig. 1C; Table S2), the Δ*liaR* mutant showed nearly identical virulence to

that of the parental strain in survival and CFU recovery from muscle tissues (Fig. 4A and B).

Transcriptome data show significantly increased *speB* transcription attributable to the reduced SpxA2 levels in the Δ*liaR* isogenic mutant strain (Fig. 1D). Previous studies have shown the importance of SpeB in GAS virulence, including regulation by RopB (29). We hypothesized that the lack of reduced virulence in the Δ*liaR* mutant compared to that in the parental strain in the *in vivo* mouse model may be attributable to excess SpeB. To test this hypothesis, mice were infected intramuscularly with the Δ*liaR* Δ*ropB* mutant and monitored for survival and CFU determination. We observed significantly increased survival in mice infected with the Δ*liaR* Δ*ropB* mutant compared to those infected with the parental (Δ*liaR*) or wild-type (MGAS10870) strains (Fig. 4A). Similarly, bacterial burden in infected tissue at 48 h was reduced for the mutant lacking *ropB* compared to either the Δ*liaR* or wild-type strain (Fig. 4B). Thus, in the absence of increased *speB* expression, the Δ*liaR* mutant shows significantly reduced virulence in a mouse model of invasive GAS disease.

Our previous studies showed a codependence between LiaF and the GAS ExPortal (19). ExPortal disruption resulted in LiaF dissociation, activation of LiaS, and LiaR phosphorylation. However, in the absence of LiaF (Δ*liaF*), the ExPortal integrity was compromised, indicating that a Δ*liaF* mutant may have reduced fitness *in vivo* (19). Furthermore, LiaFSR and the GAS ExPortal respond specifically to the human AMP hNP-1, an alpha-defensin (19, 30). In mice, alpha-defensins are only expressed in the Paneth cells of the intestines and not in neutrophils (31). Thus, we hypothesized that loss of the GAS ExPortal in the Δ*liaF* mutant results in decreased fitness, secondary to loss of the ability to respond to human AMPs, that cannot be overcome by *ex vivo* or *in vitro* stimulation. We first performed bactericidal assays of parental and isogenic mutant strains using human blood *ex vivo* (2 independent adult donors). In contrast to the *in vivo* mouse model, we observed significantly reduced ability of the Δ*liaR* mutant to survive in human blood despite the overproduction of SpeB (Fig. 4C). However, as seen in the mouse model, following exposure to human blood *ex vivo*, the Δ*liaF* mutant showed significantly reduced survival (Fig. 4C), suggesting a significant fitness cost to ExPortal disruption. It is estimated that 10^6 neutrophils (approximately 1 ml of blood) contain >5 μg of hNP-1 (32). Given the critical importance of LiaFSR and the ExPortal in sensing hNP-1, we next hypothesized that *in vitro* exposure to hNP-1 would reveal virulence gene dysregulation secondary to LiaFSR or ExPortal dysfunction in the Δ*liaR* or Δ*liaF* mutant, respectively. We assayed target gene transcription in parental and isogenic mutant strains following treatment with identical concentrations of hNP-1 previously shown to disrupt the ExPortal and activate LiaFSR (19). Following stimulation with hNP-1, the parental strain showed significant increases in *spxA2*, *hasA*, and *mac-1* transcripts (Fig. 4D). In contrast, compared to the wild type (WT) treated with hNP-1, the Δ*liaR* strain showed significant dysregulation of gene transcription and reduction of gene transcription (Fig. 4E). Following stimulation with hNP-1, the Δ*liaF* mutant showed transcript levels of *spxA2*, *hasA*, and *mac-1* similar to those in the WT stimulated with hNP-1 (Fig. 4E), suggesting a mechanism independent of LiaFSR (e.g., loss of ExPortal integrity) contributing to decreased virulence. Together, these data suggest that the LiaFSR regulatory system and the ExPortal are essential for proper virulence gene expression in response to exogenous host stresses.

DISCUSSION

We originally described a single amino acid replacement in the HK, LiaS, of the LiaFSR system in GAS that contributed to asymptomatic carriage and persistence following acute symptomatic pharyngitis in a human subject (33). The mechanism by which the carrier mutation altered virulence was through a trade-off between decreased ability to cause disease and increased ability to adhere to mucosal surfaces (23). Most recently, we expanded our studies to show that the inhibitory protein, LiaF, and LiaS reside within the GAS ExPortal and that human AMP-mediated disruption

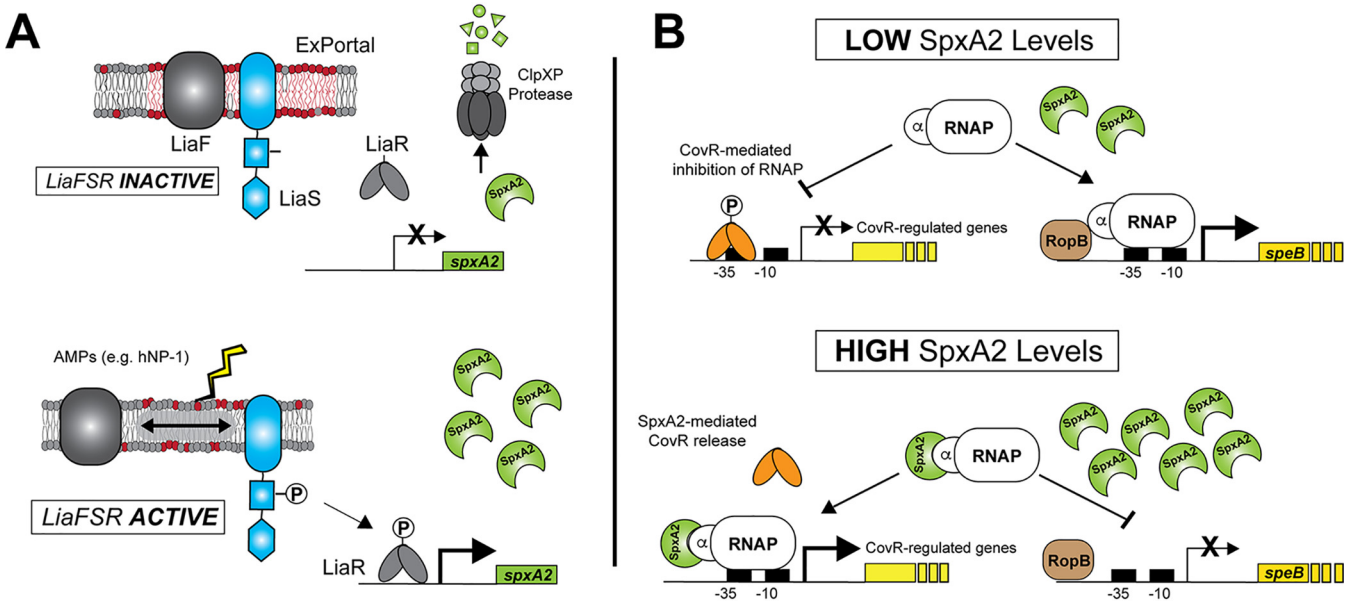

FIG 5 Model of SpxA2-mediated CovR-regulated gene expression in GAS. (A) Previous studies (19) showed an intimate relationship between the GAS ExPortal, LiaF, and LiaS. Under nonactivating conditions, SpxA2 is rapidly degraded by the ClpXP protease. Disruption of the ExPortal through antimicrobials or antimicrobial peptides (e.g., hNP-1) lead to LiaF/LiaS dissociation and activation of the LiaFSR system (i.e., LiaR phosphorylation [LiaR~P]). Our data support direct binding of LiaR~P to the promoter of *spxA2*, resulting in increased SpxA2 protein—a protein known to alter transcription through direct interaction with the alpha subunit of RNA polymerase (RNAP) (20). (B) When SpxA2 levels are low, GAS cells produce greater amounts of SpeB protease, presumably through increased interaction of RNAP with RopB (regulatory of SpeB expression) (22). In contrast to *speB* regulation, our data indicate that low-SpxA2 conditions contribute to CovR-regulated gene repression (decreased transcription). However, upon activation of LiaFSR, increased *spxA2* transcription leads to increases in the intracellular SpxA2 pool and binding of SpxA2 to RNAP to decrease *speB* and increase CovR-regulated gene transcription. Thus, SpxA2 may act to alter the regulatory tone of the cell in a regulator- and/or promoter-dependent manner.

leads to ExPortal disruption and dissociation of LiaF/LiaS to activate the LiaFSR system (19). The present study adds greater clarity to the downstream effects following LiaFSR activation. Our data support the concept that activation of LiaFSR and subsequent LiaR phosphorylation lead directly to increased *spxA2* transcription that further serves to expand gene regulation to include multiple regulatory networks. Furthermore, the observed paradoxical virulence phenotypes may be indicative of complex gene regulatory system interaction that results from both ExPortal disruption and LiaFSR activation.

Activation of the LiaFSR system directly influences transcription of *spxA2* in GAS, and disruption of LiaFSR activation negatively affects virulence. Two Spx homologs exist in pathogenic streptococci, including GAS, GBS, and *S. mutans*. In *S. mutans*, both SpxA1 and SpxA2 are required for caries formation in a rat model (34). Furthermore, LiaR was shown to bind the *spxA1* (GAS SpxA2 homolog) promoter in *S. mutans* (24), leading to increased SpxA1 and facilitating the response to cell envelope stress (35). Evidence for LiaR regulation of SpxA in GBS comes from a transcriptome analysis of a LiaR deletion mutant showing that in the absence of LiaR, SpxA (SAK_2031 in strain A909), transcription is decreased >26-fold (25). The conserved nature of SpxA1/2 in streptococci suggests a common mechanism by which this group of organisms responds to cell envelope stress. Likewise, by binding directly to RNA polymerase, Spx proteins may have a very broad effect on gene transcription, contributing to the cell regulatory tone and providing a unique system of regulatory network cross talk. Our data indicate a direct correlation between SpxA2 levels and virulence gene transcription that may be secondary to interference with CovR-mediated virulence gene repression—similar to the rationale provided for interference with RopB-regulated *speB* transcription in GAS (22). That is, high levels of SpxA2 (via increased transcription or resistance to degradation in oxidative stress) and binding to RNA polymerase appear to alter gene expression through RopB, CovR, and very likely other transcription factors (Fig. 5).

At first glance, our data appear to be in contrast to the prior studies examining SpxA2 and effects on GAS virulence (22). Absence of SpxA2 was previously shown to increase the ability of GAS bacteria to cause disease in a mouse subcutaneous infection model and was entirely dependent upon excess SpeB production (22). In this regard, our data are consistent in that the Δ*liaR* mutant (low SpxA2, high SpeB) showed similar virulence and a modest but insignificant increase in bacterial burden despite marked reduction in transcription for multiple virulence factors—a phenotype in contrast to our expectation but dependent upon excess SpeB production. Thus, our data are not only consistent with previous observations but add substantially to our understanding of gene regulation of and through SpxA2. Our findings suggest that by altering levels of SpxA2, the LiaFSR system serves to modulate the regulatory tone of the GAS cell with potential consequences in multiple regulatory networks.

Surprisingly, the Δ*liaF* mutant demonstrated significantly reduced virulence in both *in vivo* and *ex vivo* models of GAS disease. The mechanism by which LiaF contributes to ExPortal stability is unknown, but given the known excess relative to its partner, LiaS, in *Bacillus* (36), LiaF may serve as a scaffolding protein similar to flotillins (37). Our data demonstrate that an "always on" LiaFSR transcriptome in the Δ*liaF* mutant is unable to overcome the loss of ExPortal integrity. In addition to the loss of SpeB, it is possible that loss of ExPortal function in the Δ*liaF* mutant may alter protein localization and other gene regulatory networks, resulting in an inability to appropriately respond to AMP exposure. Support for this hypothesis comes from studies in *Staphylococcus aureus* showing that multiple TCS HKs are enriched within FMMs (37), suggesting that the FMM/ExPortal may act as a "command center" and contributes to regulatory system cross talk. For example, in addition to the *S. aureus* LiaS homolog (VraS), GraS and SaeS have also been shown to be enriched in the *S. aureus* FMM (37). Importantly, both GraS and SaeS are known to be critical to survival in professional phagocytes such as macrophages (38) or neutrophils (39, 40). It was previously shown that the Ihk/Irr TCS of GAS was essential for neutrophil survival (41, 42). Given the specificity of ExPortal disruption and LiaFSR activation following exposure to hNP-1 (19, 30), it is tempting to speculate that Ihk or other GAS TCSs may reside within the GAS ExPortal as a means to sense the host environment and respond accordingly. The protein content of the GAS ExPortal is largely unknown, and additional work is needed to determine if virulence regulatory systems are similarly located in the GAS ExPortal and to determine their role in sensing through this critical structure.

In summary, our studies provide a greater understanding of the nature of LiaFSR in the GAS cell envelope response. Gene regulatory changes following ExPortal disruption and activation of LiaFSR are complex, consisting of regulatory system cross talk mediated by SpxA2. The highly conserved nature of LiaFSR and SpxA2 in Gram-positive bacteria suggests a common mechanism by which these human pathogens respond to host molecules.

MATERIALS AND METHODS

Bacterial strains and culture conditions. Strains used in this study are listed in Table S3 in the supplemental material. MGAS10870 is a serotype M3 GAS isolated in ON, Canada, in 2002 from a patient with a soft tissue infection (43) and was the wild-type strain used in this study. All GAS strains were grown at 37°C in Todd-Hewitt broth containing 0.2% (wt/vol) yeast extract (THY; Difco Laboratories), on THY agar, or on BD Trypticase soy agar II with 5% sheep blood (Becton, Dickinson). Liquid cultures and solid cultures were incubated at 37°C with 5% CO_2. In selected experiments, growth medium was supplemented with bacitracin (1 μg/ml) (Sigma-Aldrich) and human neutrophil peptide-1 (100 μg/ml) (hNP-1; AnaSpec) or diamide (Sigma-Aldrich). Cloning for generation of GAS mutants was performed in *Escherichia coli* NEB5alpha (New England BioLabs) grown in Luria-Bertani (LB; Becton, Dickinson) broth or LB agar plates. When needed, spectinomycin (Sigma-Aldrich) or kanamycin (Sigma-Aldrich) was added to media for the growth of GAS and *E. coli*.

Generation of genomic mutant strains in MGAS10870. Mutants generated in this study are listed in Table S3. Isogenic insertional inactivation mutants of *liaF*, *liaR*, and *ropB* were identical to those used in our previous study (19). Similarly, isogenic deletion mutants for *clpX* and *spxA2* were made by in-frame insertional inactivation with a spectinomycin resistance gene (*aad9*) or kanamycin resistance gene (*aph*) using pJL1055, as previously described (44). Primers and plasmids used in cloning for mutant generation are listed in Table S4. Isogenic mutant gene replacement and lack of spurious mutations were confirmed

using whole-genome sequencing. Briefly, DNA extraction, library preparation, sequencing using an Illumina MiSeq instrument (300-bp, paired-end), and analysis were performed as previously described (45). The minimum depth of coverage was >50×, and no spurious mutations were identified relative to the wild-type strain.

RNA isolation and qRT-PCR analysis. Cell growth was performed as described above. Cultures were harvested by centrifugation following the addition of RNAprotect bacterial reagent (Qiagen), and RNA was isolated and purified with an RNeasy minikit (Qiagen) according to the protocol for Gram-positive bacteria. The quantity and quality of RNA were determined using a NanoDrop (Thermo Fisher) and an Agilent 4200 TapeStation system (Agilent Technologies). TaqMan (Applied Biosystems) quantitative real-time PCR (qRT-PCR) of cDNA generated using SuperScript III reverse transcriptase (Invitrogen) was performed with an CFX96 Touch real-time PCR detection system (Bio-Rad) according to the manufacturer's instructions. The TaqMan primers and probes used in the analyses are listed in Table S4. Transcript levels of genes were calculated by relative quantification using the comparative threshold cycle ($\Delta\Delta C_T$) method as described previously (46), with an internal reference gene *tufA* as the normalizing gene. All reactions were performed in triplicates using RNA purified from at least three biological replicates.

Chromatin immunoprecipitation qRT-PCR. GAS cultures were grown to mid-exponential phase (OD_{600} of ~1.0) in THY as described above. Formaldehyde (Sigma-Aldrich) was added to obtain a 1% final concentration, and cultures were shaken at room temperature for 8 min. Glycine (Sigma-Aldrich) was added to obtain a 0.125 M concentration and incubated at room temperature for 10 min. Cells were harvested, washed with phosphate-buffered saline (PBS) and flash frozen in liquid nitrogen. Cell lysis was performed using a Bioruptor Pico (Diagenode), and lysates were incubated with magnetic beads coupled with anti-LiaR antibody (19) for 24 h. Immunoprecipitated DNA was purified and used in qRT-PCRs using probes and primers for *spxA* motifs and *tufA* (Table S4). Individual strains were repeated in biological triplicates.

RNA sequencing and analysis. GAS strains were grown in THY broth (biological quadruplicates) to exponential phase (OD_{600} of ~1.0), and cells were harvested by centrifugation identically to that described for real-time PCR analysis. RNA isolation, RNA purification, rRNA depletion, and development of adapter-tagged cDNA libraries were performed using a Script-Seq Complete kit (bacteria) (Epicentre [Illumina]). cDNA libraries were run on an Illumina HiSeq 4000, and an average of ~62 million (range, 48 to 77 million) 150-bp paired-end reads were obtained per replicate sample. Following on-board adapter trimming and quality control, reads were subsequently mapped to the reference serotype M3 genome (MGAS10870) using CLC Genomics Workbench version 20 (Qiagen). Identification of significantly differentially expressed genes was determined as we have previously described (47, 48). Genes for which the change in expression was ≥1.5-fold and *P* value was <0.05 following Bonferroni's correction for multiple comparisons were considered to have a significant difference in expression.

Detection of LiaR and CovR phosphorylation levels *in vivo*. CovR phosphorylation levels were measured as described previously (19, 49). Briefly, GAS cells were lysed using a FastPrep-24 5G homogenizer (MP Biomedicals), and lysates were separated on 12.5% SuperSeq Phos-Tag gels (Wako, USA). Un/phosphorylated CovR species were detected using a polyclonal anti-CovR antibody and the Odyssey imaging system. Strains were analyzed on a minimum of 2 independent biological replicates.

Mouse intramuscular infection. All animal experiments were conducted under a protocol approved by the UTHealth Institutional Animal Care and Use Committee. CD1 mice (Charles River, 3 to 4 weeks of age, male and female) were inoculated in the right hind limb with 5×10^7 CFU of the appropriate GAS strain in 50 μl of phosphate-buffered saline (PBS). For survival, infected mice (n = 15 per strain group) were observed and euthanized when they reached near mortality determined using predefined criteria. For bacterial burden, mice (n = 20 mice per strain group) were euthanized, the infected limbs were homogenized, and the lysates were serially diluted in sterile PBS and plated on 5% Sabouraud agar (SBA) to enumerate GAS bacteria. Final CFU were normalized by limb weight (CFU/g tissue).

***Ex vivo* bactericidal assays in human blood.** Growth in whole human blood was conducted under an experimental protocol approved by the UTHealth Committee for the Protection of Human Subjects and performed as described by Lancefield (50). Blood from a minimum of two, healthy, nonimmune adult donors was used for each experiment.

Statistics. All statistical analyses were performed in Prism 9 (GraphPad Software, Inc.). The data shown represent the means ± standard deviations (SDs) from biological replicates. Differences between mean values were tested for significance with a two-tailed Student's *t* test, Mann-Whitney U test (nonparametric data), and statistical difference was set at a *P* value of <0.05 for all comparisons.

Data availability. The RNAseq data have been deposited in the NCBI GEO database under accession number GSE181516.

SUPPLEMENTAL MATERIAL

Supplemental material is available online only.

SUPPLEMENTAL FILE 1, PDF file, 0.1 MB.

SUPPLEMENTAL FILE 2, PDF file, 0.2 MB.

ACKNOWLEDGMENTS

This work was supported by funding provided by the National Institute of Allergy and Infectious Diseases R01 AI124216 (A.R.F.) and T32 AI141349 (L.A.V.).

REFERENCES

1. Carapetis JR. 2005. Current evidence for the burden of Group A streptococcal diseases. World Health Organization, Geneva, Switzerland.
2. Nelson GE, Pondo T, Toews KA, Farley MM, Lindegren ML, Lynfield R, Aragon D, Zansky SM, Watt JP, Cieslak PR, Angeles K, Harrison LH, Petit S, Beall B, Van Beneden CA. 2016. Epidemiology of invasive group A streptococcal infections in the United States, 2005–2012. Clin Infect Dis 63:478–486. https://doi.org/10.1093/cid/ciw248.
3. O'Loughlin RE, Roberson A, Cieslak PR, Lynfield R, Gershman K, Craig A, Albanese BA, Farley MM, Barrett NL, Spina NL, Beall B, Harrison LH, Reingold A, Van Beneden C, Active Bacterial Core Surveillance Team. 2007. The epidemiology of invasive group A streptococcal infection and potential vaccine implications: united States, 2000–2004. Clin Infect Dis 45:853–862. https://doi.org/10.1086/521264.
4. Valenciano SJ, Onukwube J, Spiller MW, Thomas A, Como-Sabetti K, Schaffner W, Farley M, Petit S, Watt JP, Spina N, Harrison LH, Alden NB, Torres S, Arvay ML, Beall B, Van Beneden CA. 17 June 2020. Invasive group A streptococcal infections among people who inject drugs and people experiencing homelessness in the United States. Clin Infect Dis https://doi.org/10.1093/cid/ciaa787.
5. Vega LA, Malke H, McIver KS. 2016. Virulence-related transcriptional regulators of *Streptococcus pyogenes*. *In* Ferretti JJ, Stevens DL, Fischetti VA (ed), *Streptococcus pyogenes:* basic biology to clinical manifestations. University of Oklahoma Health Sciences Center, Oklahoma City, OK.
6. Stock AM, Robinson VL, Goudreau PN. 2000. Two-component signal transduction. Annu Rev Biochem 69:183–215. https://doi.org/10.1146/annurev.biochem.69.1.183.
7. Churchward G. 2007. The two faces of Janus: virulence gene regulation by CovR/S in group A streptococci. Mol Microbiol 64:34–41. https://doi.org/10.1111/j.1365-2958.2007.05649.x.
8. Levin JC, Wessels MR. 1998. Identification of *csrR/csrS*, a genetic locus that regulates hyaluronic acid capsule synthesis in group A *Streptococcus*. Mol Microbiol 30:209–219. https://doi.org/10.1046/j.1365-2958.1998.01057.x.
9. Gryllos I, Levin JC, Wessels MR. 2003. The CsrR/CsrS two-component system of group A *Streptococcus* responds to environmental Mg^{2+}. Proc Natl Acad Sci U S A 100:4227–4232. https://doi.org/10.1073/pnas.0636231100.
10. Gryllos I, Tran-Winkler HJ, Cheng MF, Chung H, Bolcome R, III, Lu W, Lehrer RI, Wessels MR. 2008. Induction of group A *Streptococcus* virulence by a human antimicrobial peptide. Proc Natl Acad Sci U S A 105:16755–16760. https://doi.org/10.1073/pnas.0803815105.
11. Flores AR, Luna RA, Runge JK, Shelburne SA, III, Baker CJ. 2017. Cluster of fatal group A streptococcal *emm87* infections in a single family: molecular basis for invasion and transmission. J Infect Dis 215:1648–1652. https://doi.org/10.1093/infdis/jix177.
12. Liu G, Feng W, Li D, Liu M, Nelson DC, Lei B. 2015. The Mga regulon but not deoxyribonuclease Sda1 of invasive M1T1 group A *Streptococcus* contributes to *in vivo* selection of CovRS mutations and resistance to innate immune killing mechanisms. Infect Immun 83:4293–4303. https://doi.org/10.1128/IAI.00857-15.
13. Walker MJ, Hollands A, Sanderson-Smith ML, Cole JN, Kirk JK, Henningham A, McArthur JD, Dinkla K, Aziz RK, Kansal RG, Simpson AJ, Buchanan JT, Chhatwal GS, Kotb M, Nizet V. 2007. DNase Sda1 provides selection pressure for a switch to invasive group A streptococcal infection. Nat Med 13:981–985. https://doi.org/10.1038/nm1612.
14. Arias CA, Panesso D, McGrath DM, Qin X, Mojica MF, Miller C, Diaz L, Tran TT, Rincon S, Barbu EM, Reyes J, Roh JH, Lobos E, Sodergren E, Pasqualini R, Arap W, Quinn JP, Shamoo Y, Murray BE, Weinstock GM. 2011. Genetic basis for in vivo daptomycin resistance in enterococci. N Engl J Med 365:892–900. https://doi.org/10.1056/NEJMoa1011138.
15. Munita JM, Tran TT, Diaz L, Panesso D, Reyes J, Murray BE, Arias CA. 2013. A *liaF* codon deletion abolishes daptomycin bactericidal activity against vancomycin-resistant *Enterococcus faecalis*. Antimicrob Agents Chemother 57:2831–2833. https://doi.org/10.1128/AAC.00021-13.
16. Jordan S, Hutchings MI, Mascher T. 2008. Cell envelope stress response in Gram-positive bacteria. FEMS Microbiol Rev 32:107–146. https://doi.org/10.1111/j.1574-6976.2007.00091.x.
17. Boyle-Vavra S, Yin S, Jo DS, Montgomery CP, Daum RS. 2013. VraT/YvqF is required for methicillin resistance and activation of the VraSR regulon in *Staphylococcus aureus*. Antimicrob Agents Chemother 57:83–95. https://doi.org/10.1128/AAC.01651-12.
18. Jordan S, Junker A, Helmann JD, Mascher T. 2006. Regulation of LiaRS-dependent gene expression in bacillus subtilis: identification of inhibitor proteins, regulator binding sites, and target genes of a conserved cell envelope stress-sensing two-component system. J Bacteriol 188:5153–5166. https://doi.org/10.1128/JB.00310-06.
19. Lin Y, Sanson MA, Vega LA, Shah B, Regmi S, Cubria MB, Flores AR. 2020. ExPortal and the LiaFSR regulatory system coordinate the response to cell membrane stress in *Streptococcus pyogenes*. mBio 11:e01804-20. https://doi.org/10.1128/mBio.01804-20.
20. Zuber P. 2004. Spx-RNA polymerase interaction and global transcriptional control during oxidative stress. J Bacteriol 186:1911–1918. https://doi.org/10.1128/JB.186.7.1911-1918.2004.
21. Nakano MM, Hajarizadeh F, Zhu Y, Zuber P. 2001. Loss-of-function mutations in *yjbD* result in ClpX- and ClpP-independent competence development of *Bacillus subtilis*. Mol Microbiol 42:383–394. https://doi.org/10.1046/j.1365-2958.2001.02639.x.
22. Port GC, Cusumano ZT, Tumminello PR, Caparon MG. 2017. SpxA1 and SpxA2 act coordinately to fine-tune stress responses and virulence in *Streptococcus pyogenes*. mBio 8:e00288-17. https://doi.org/10.1128/mBio.00288-17.
23. Flores AR, Olsen RJ, Cantu C, Pallister KB, Guerra FE, Voyich JM, Musser JM. 2017. Increased pilus production conferred by a naturally occurring mutation alters host-pathogen interaction in favor of carriage in *Streptococcus pyogenes*. Infect Immun 85:e00949-16. https://doi.org/10.1128/IAI.00949-16.
24. Shankar M, Mohapatra SS, Biswas S, Biswas I. 2015. Gene regulation by the LiaSR two-component system in *Streptococcus mutans*. PLoS One 10:e0128083. https://doi.org/10.1371/journal.pone.0128083.
25. Klinzing DC, Ishmael N, Hotopp JCD, Tettelin H, Shields KR, Madoff LC, Puopolo KM. 2013. The two-component response regulator LiaR regulates cell wall stress responses, pili expression and virulence in group B *Streptococcus*. Microbiology (Reading) 159:1521–1534. https://doi.org/10.1099/mic.0.064444-0.
26. Bailey TL, Johnson J, Grant CE, Noble WS. 2015. The MEME Suite. Nucleic Acids Res 43:W39–W49. https://doi.org/10.1093/nar/gkv416.
27. Kosower NS, Kosower EM. 1995. Diamide: an oxidant probe for thiols. Methods Enzymol 251:123–133. https://doi.org/10.1016/0076-6879(95)51116-4.
28. Olsen RJ, Sitkiewicz I, Ayeras AA, Gonulal VE, Cantu C, Beres SB, Green NM, Lei B, Humbird T, Greaver J, Chang E, Ragasa WP, Montgomery CA, Cartwright J, Jr, McGeer A, Low DE, Whitney AR, Cagle PT, Blasdel TL, DeLeo FR, Musser JM. 2010. Decreased necrotizing fasciitis capacity caused by a single nucleotide mutation that alters a multiple gene virulence axis. Proc Natl Acad Sci U S A 107:888–893. https://doi.org/10.1073/pnas.0911811107.
29. Carroll RK, Shelburne SA, III, Olsen RJ, Suber B, Sahasrabhojane P, Kumaraswami M, Beres SB, Shea PR, Flores AR, Musser JM. 2011. Naturally occurring single amino acid replacements in a regulatory protein alter streptococcal gene expression and virulence in mice. J Clin Invest 121:1956–1968. https://doi.org/10.1172/JCI45169.
30. Vega LA, Caparon MG. 2012. Cationic antimicrobial peptides disrupt the *Streptococcus pyogenes* ExPortal. Mol Microbiol 85:1119–1132. https://doi.org/10.1111/j.1365-2958.2012.08163.x.
31. Eisenhauer PB, Lehrer RI. 1992. Mouse neutrophils lack defensins. Infect Immun 60:3446–3447. https://doi.org/10.1128/iai.60.8.3446-3447.1992.
32. Ganz T. 1987. Extracellular release of antimicrobial defensins by human polymorphonuclear leukocytes. Infect Immun 55:568–571. https://doi.org/10.1128/iai.55.3.568-571.1987.
33. Flores AR, Jewell BE, Yelamanchili D, Olsen RJ, Musser JM. 2015. A single amino acid replacement in the sensor kinase LiaS contributes to a carrier phenotype in group A *Streptococcus*. Infect Immun 83:4237–4246. https://doi.org/10.1128/IAI.00656-15.
34. Galvao LC, Rosalen PL, Rivera-Ramos I, Franco GC, Kajfasz JK, Abranches J, Bueno-Silva B, Koo H, Lemos JA. 2017. Inactivation of the *spxA1* or *spxA2* gene of *Streptococcus mutans* decreases virulence in the rat caries model. Mol Oral Microbiol 32:142–153. https://doi.org/10.1111/omi.12160.
35. Baker JL, Saputo S, Faustoferri RC, Quivey RG, Jr. 2020. *Streptococcus mutans* SpxA2 relays the signal of cell envelope stress from LiaR to effectors that maintain cell wall and membrane homeostasis. Mol Oral Microbiol 35:118–128. https://doi.org/10.1111/omi.12282.
36. Schrecke K, Jordan S, Mascher T. 2013. Stoichiometry and perturbation studies of the LiaFSR system of *Bacillus subtilis*. Mol Microbiol 87:769–788. https://doi.org/10.1111/mmi.12130.
37. Garcia-Fernandez E, Koch G, Wagner RM, Fekete A, Stengel ST, Schneider J, Mielich-Suss B, Geibel S, Markert SM, Stigloher C, Lopez D. 2017. Membrane

microdomain disassembly inhibits MRSA antibiotic resistance. Cell 171:1354–1367 e20. https://doi.org/10.1016/j.cell.2017.10.012.
38. Flannagan RS, Kuiack RC, McGavin MJ, Heinrichs DE. 2018. *Staphylococcus aureus* uses the GraXRS regulatory system to sense and adapt to the acidified phagolysosome in macrophages. mBio 9:e01143-18. https://doi.org/10.1128/mBio.01143-18.
39. Guerra FE, Addison CB, de Jong NW, Azzolino J, Pallister KB, van Strijp JA, Voyich JM. 2016. *Staphylococcus aureus* SaeR/S-regulated factors reduce human neutrophil reactive oxygen species production. J Leukoc Biol 100:1005–1010. https://doi.org/10.1189/jlb.4VMAB0316-100RR.
40. Sward EW, Fones EM, Spaan RR, Pallister KB, Haller BL, Guerra FE, Zurek OW, Nygaard TK, Voyich JM. 2018. *Staphylococcus aureus* SaeR/S-regulated factors decrease monocyte-derived tumor necrosis factor-alpha to reduce neutrophil bactericidal activity. J Infect Dis 217:943–952. https://doi.org/10.1093/infdis/jix652.
41. Voyich JM, Braughton KR, Sturdevant DE, Vuong C, Kobayashi SD, Porcella SF, Otto M, Musser JM, DeLeo FR. 2004. Engagement of the pathogen survival response used by group A *Streptococcus* to avert destruction by innate host defense. J Immunol 173:1194–1201. https://doi.org/10.4049/jimmunol.173.2.1194.
42. Voyich JM, Sturdevant DE, Braughton KR, Kobayashi SD, Lei B, Virtaneva K, Dorward DW, Musser JM, DeLeo FR. 2003. Genome-wide protective response used by group A *Streptococcus* to evade destruction by human polymorphonuclear leukocytes. Proc Natl Acad Sci U S A 100:1996–2001. https://doi.org/10.1073/pnas.0337370100.
43. Beres SB, Carroll RK, Shea PR, Sitkiewicz I, Martinez-Gutierrez JC, Low DE, McGeer A, Willey BM, Green K, Tyrrell GJ, Goldman TD, Feldgarden M, Birren BW, Fofanov Y, Boos J, Wheaton WD, Honisch C, Musser JM. 2010. Molecular complexity of successive bacterial epidemics deconvoluted by comparative pathogenomics. Proc Natl Acad Sci U S A 107:4371–4376. https://doi.org/10.1073/pnas.0911295107.
44. Li J, Kasper DL, Ausubel FM, Rosner B, Michel JL. 1997. Inactivation of the alpha C protein antigen gene, *bca*, by a novel shuttle/suicide vector results in attenuation of virulence and immunity in group B *Streptococcus*. Proc Natl Acad Sci U S A 94:13251–13256. https://doi.org/10.1073/pnas.94.24.13251.
45. Sanson MA, Macias OR, Shah BJ, Hanson B, Vega LA, Alamarat Z, Flores AR. 2019. Unexpected relationships between frequency of antimicrobial resistance, disease phenotype and emm type in group A *Streptococcus*. Microb Genom 5:e000316. https://doi.org/10.1099/mgen.0.000316.
46. Livak KJ, Schmittgen TD. 2001. Analysis of relative gene expression data using real-time quantitative PCR and the 2(-Delta Delta C(T)) method. Methods 25:402–408. https://doi.org/10.1006/meth.2001.1262.
47. DebRoy S, Aliaga-Tobar V, Galvez G, Arora S, Liang X, Horstmann N, Maracaja-Coutinho V, Latorre M, Hook M, Flores AR, Shelburne SA. 2020. Genome-wide analysis of *in vivo* CcpA binding with and without its key co-factor HPr in the major human pathogen group A *Streptococcus*. Mol Microbiol 115:1207–1228. https://doi.org/10.1111/mmi.14667.
48. Sanson M, Flores AR. 2020. Group A *Streptococcus* transcriptome analysis. Methods Mol Biol 2136:113–133. https://doi.org/10.1007/978-1-0716-0467-0_8.
49. Horstmann N, Sahasrabhojane P, Saldana M, Ajami NJ, Flores AR, Sumby P, Liu CG, Yao H, Su X, Thompson E, Shelburne SA. 2015. Characterization of the effect of the histidine kinase CovS on response regulator phosphorylation in group A *Streptococcus*. Infect Immun 83:1068–1077. https://doi.org/10.1128/IAI.02659-14.
50. Lancefield RC. 1957. Differentiation of group A streptococci with a common R antigen into three serological types, with special reference to the bactericidal test. J Exp Med 106:525–544. https://doi.org/10.1084/jem.106.4.525.